Fuel 267 (2020) 117155

Contents lists available at ScienceDirect

Fuel

journal homepage: www.elsevier.com/locate/fuel

Full Length Article

Swelling of Kimmeridge kerogen by normal-alkanes, naphthenes and aromatics

Liang Huang[a,b,c,d,e], Atefeh Khoshnood[e], Abbas Firoozabadi[e,f,*]

[a] College of Energy, Chengdu University of Technology, Chengdu, Sichuan 610059, PR China
[b] State Key Laboratory of Oil and Gas Reservoir Geology and Exploitation, Chengdu University of Technology, Chengdu, Sichuan 610059, PR China
[c] State Key Laboratory of Petroleum Resources and Prospecting, China University of Petroleum (Beijing), Beijing 102249, PR China
[d] Department of Chemical and Biomolecular Engineering, University of California, Berkeley, Berkeley, CA 94720-1462, USA
[e] Reservoir Engineering Research Institute, 595 Lytton Avenue, Suite B., Palo Alto, CA 94301, USA
[f] Department of Chemical and Biomolecular Engineering, Rice University, Houston, TX 77005, USA

ARTICLE INFO

Keywords:
Swelling
Kerogen
Petroleum liquids
Molecular size

ABSTRACT

Despite recognition of kerogen swelling in liquid solvents, swelling trends in different classes of petroleum liquids remain unexplored. Modeling results based on the extended polymer theory have not been beyond curve-fitting of swelling measurements. This work centers on measurement of swelling of Kimmeridge kerogen in three classes of petroleum liquids: normal-alkanes, naphthenes and aromatics. The measured data show that swelling decreases as the molecular size increases for the three classes of solvents. Compared with naphthenes, normal-alkanes with flexible linear chains, and aromatics having π–π interaction with kerogen induce higher swelling. In the Kimmeridge kerogen, the swelling in both normal-alkanes and naphthenes monotonously decreases with the solvent solubility parameter and molar volume starting with hydrocarbon molecules with 5 carbon atoms. Compared with solvent solubility parameter, the effect of solvent molar volume dominates the swelling of Kimmeridge kerogen. The extended Flory-Rehner and regular solution theory framework does not describe the swelling behavior of Kimmeridge kerogen in petroleum liquids despite widespread applications of the framework. Results from the model show an increase in swelling in normal alkanes with molecular size which is opposite to our measurements.

1. Introduction

Petroleum fluids are generated from the organic matter of shale. The organic matter which often consists of kerogen has a cross-linked network with a complex molecular structure [1]. The maturation of kerogen includes both the bond-breaking and bond-making reactions. The bond-breaking reactions lead to the conversion of organic carbon in kerogen skeleton into volatile hydrocarbons, bitumen and solid residue [2]; the bond-making reactions contribute to the increase of the cross-linked degree of the organic network [3]. Kerogen has abundant nanopores and large specific surface areas, which facilitates the storage of the generated hydrocarbons [4,5]. Expulsion of petroleum hydrocarbons, also called primary migration, is the initial stage of petroleum migration from the source kerogen to the reservoir accumulation. The process remains poorly understood [6,7]. Kerogen is in dynamic equilibrium with the generated hydrocarbons during the expulsion process.

The producible hydrocarbon and non-hydrocarbon species are in three states in kerogen: free molecules in the pores, adsorbed molecules on the surfaces and dissolved molecules in the kerogen network [8]. The expulsion process is accompanied by chemical fractionation where saturated hydrocarbons and aromatics are preferentially expelled compared to polar compounds and polycyclic aromatic hydrocarbons such as asphaltenes and resins [6,7]. There have been many investigations on the chemical fractionation during expulsion [6,7,9–15]. These investigations have emphasized the role of either the pairwise interaction or the solubility difference between solvents and organic network. The mechanisms provide the process direction but not magnitude of the chemical fractionation [15]. Physical principles like the effect of fluid molecular size on the chemical fractionation remain less understood than chemical principles.

Kerogen is a soft nanoporous matter with flexible molecular structure [16–18]. The generated petroleum compounds when dissolved in kerogen matrix may induce the swelling of kerogen. Swelling of the kerogen network by different liquid solvents is well-known; it may be used to characterize its physical structure and chemical nature [3,6]. Swelling of kerogen immersed in various liquid solvents has been

* Corresponding author.
E-mail address: af@rerinst.org (A. Firoozabadi).

https://doi.org/10.1016/j.fuel.2020.117155
Received 11 November 2019; Received in revised form 16 January 2020; Accepted 19 January 2020
0016-2361/

measured by various authors [2,3,6,10,19–28]. A swelling as high as 47% has been reported for the Kimmeridge kerogen without bitumen extraction from exposure to heptane [29]. In addition to the effect of bitumen, the high swelling in Ref. [29] may be due to the sample preparation; the kerogen was compressed into cylindrical pellets in the swelling measurements. To the best of our knowledge, there is no comprehensive data set on the swelling of the same type of kerogen sample in various normal-alkanes, naphthenes and aromatics. In the past, liquid solvents in the same class with similar properties are selected in the swelling experiments. Measurements have also been performed on different classes of kerogen samples. No general trend of kerogen swelling of a given class of petroleum liquids has been reported to the best of our knowledge.

The regular solution theory framework has been widely adopted to describe the solubility behavior of liquid solvents in cross-linked organic materials such as polymers [30,31], coals [32,33], asphaltenes [34,35] and kerogens [22,23]. The applicability of the theory has been found to be sensitive to the type of solvent interacting with the organic materials. The basic behaviors of solvents that have nonspecific interaction with the organic materials have been assumed to follow the regular solution theory [22,23]. In contrast, the theory may not describe the behaviors of solvents that interact with the organic materials via specific interaction [31–33]. A more recent work has concluded that the regular solution theory may not describe the behavior of asphaltenes in organic solvents [35]. The nonspecific interactions are dominated by the dispersion forces. The specific interactions are exhibited when there is strong electron density or a positive charge (e.g. cation exchange) located on the bonded or nonbonded links of the interacting partners [36]. A non-classical example for a specific interaction is the hydrogen bond, which is prevalent in polymer–solvent [31] and coal-solvent systems [33].

The regular solution theory has been combined with the Flory-Rehner theory to describe swelling of kerogen immersed in solvents [3,6]. Apparent observations indicate that the swelling of kerogen in organic solvents may be described within the framework of the extended Flory-Rehner and regular solution theory framework [3,6]. These observations are based on limited solvent data. Only a small number of similar solvent groups are used in each class of petroleum hydrocarbons. Fig. 1 shows the predicted swelling of kerogen in normal-alkanes based on the theory with the fitting thermodynamic parameters of kerogen from ref [6]. The solubility parameter, cross-link density, and native swelling fraction used in the computations are 22.5 $J^{1/2}cm^{-3/2}$, 0.16 mol/cm^3 and 0.76, respectively for Type II kerogen, and 23.3 $J^{1/2}cm^{-3/2}$, 0.25 mol/cm^3 and 0.85, respectively for Type III kerogen [6]. The swelling reveals an increasing trend as the number of carbon atoms increases in normal-alkanes. One objective of this work is to provide systematic measurements on swelling of kerogen in normal alkane over a broad range to assess the applicability of the extended Flory-Rehner and regular solution theory framework. We will show that the results in Fig. 1 are not consistent with experimental data. Note that Fig. 1 is presented to examine the theoretical model using documented thermodynamic parameters. In this work, we will further assess the applicability of the theoretical model based on our experimental data in Kimmeridge kerogen, which can facilitate the improvement or development of new models in the future.

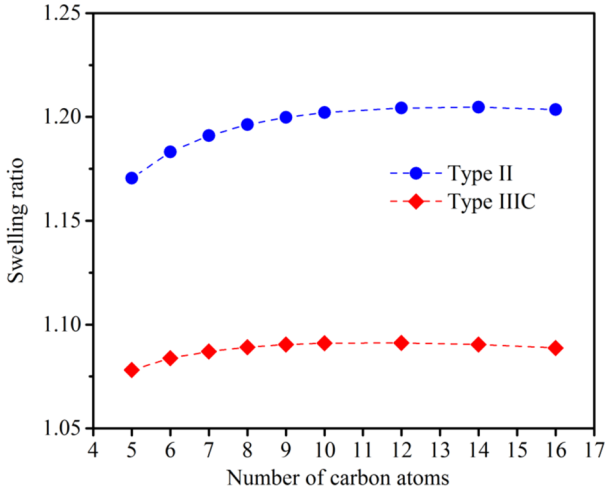

Fig. 1. Swelling ratio (volume of swelled/unswelled) of two types of kerogen as a function of number of carbon atoms in normal-alkanes. The swelling ratio is predicted by the extended Flory-Rehner and regular solution theory framework based on the thermodynamic parameters of kerogen from ref [6].

A key objective of this work is to present systematic experimental data on swelling of Kimmeridge kerogen immersed in normal-alkanes, naphthenes and aromatics. The effect of solvent solubility parameter, solvent molar volume, solvent molecular size and molecular shape on kerogen swelling will be investigated. The systematic data are used to examine the validity of the extended Flory-Rehner and regular solution theory framework in describing the swelling of kerogen. Results of this work can facilitate the development of more comprehensive mechanisms for the chemical fractionation in kerogen during petroleum expulsion.

2. Methodology

2.1. Kerogen

The shale source rock is an outcrop sampled from the Blackstone band of the Kimmeridge Clay Formation in Dorset, UK. The kerogen sample used in the swelling experiment was extracted from the source rock by acid treatment and Soxhlet extraction process. The source rock was crushed into millimeter pieces by hammer and pincer and then processed in a wig-L-bug to reduce particle size to less than 200 mesh (74 μm). A 200-mesh sieve was used to separate particles of different sizes. The sample powder was then treated with the HCl solution (6 N) to remove carbonates. The sample was kept in solution for 48 hr while the container was held in a water bath at 55 °C and magnetic mixer constantly mixed the solution. Sonication was regularly used for complete mixing. The release of CO_2 at early stage of the process showed the effectiveness of HCl to remove carbonates. At the end of treatment with HCl, the solid residue was collected by filter paper and then dried in an oven overnight at a temperature less than 60 °C. Afterwards, the HF (24 wt%) and HCl (6 N) mixture solution (1:1) was used to remove silicates in the same process as in HCl treatment. The acid concentration, acid content and interaction time with sample were designed to be sufficient to remove the silicates including clay minerals, thus eliminating the effect of clay minerals on kerogen swelling. Subsequently, the extractable organic matter was removed by Soxhlet extraction with toluene from the previous solid residue. The sample was then dried in an oven. The temperature used for drying the sample at different steps of kerogen extraction was kept below 60 °C. This is the limit that changes the maturity of the kerogen. Starting with 10 g of shale source powder, the processing of the sample resulted in ~6.5 g of kerogen powder, which indicates a high kerogen content (greater than 60%). The total organic content (TOC) of Kimmeridge kerogen is reported to be about 62.5 wt% [37]. Elemental analysis [37] shows that Kimmeridge kerogen contains 62.52 wt% carbon, 6.49 wt% hydrogen, 5.58 wt % oxygen, 1.70 wt% nitrogen and 11.31 wt% sulfur. The kerogen type corresponds to immature type II according to the hydrogen/carbon (1.25) and oxygen/carbon (0.067) atomic ratio [37].

2.2. Liquid hydrocarbons

The swelling experiments were performed in three classes of organic solvents, including normal-alkanes, intermediate naphthenes and aromatics. These liquid hydrocarbons represent the prevalent intermediate

Table 1
Measured swelling ratio of kerogen in solvents. Solubility parameter and molar volume are from [15,40].

Solvent	Solubility parameter ($J^{1/2}cm^{-3/2}$)	Molar volume (cm^3/mol)	Swelling ratio
n-pentane	14.4	114.2	1.13 ± 0.01
n-hexane	14.9	130.6	1.14 ± 0.03
n-heptane	15.2	147.0	1.11 ± 0.02
n-octane	15.5	163.4	1.06 ± 0.03
n-nonane	15.7	179.7	1.01 ± 0.03
n-decane	15.8	196.1	1.02 ± 0.01
n-dodecane	16.1	228.9	1.01 ± 0.03
n-tetradecane	16.2	261.6	1.03 ± 0.02
cyclopentane	16.4	94.7	1.14 ± 0.03
cyclohexane	16.8	108.7	1.09 ± 0.03
cycloheptane	17.2	121.3	1.07 ± 0.03
cyclooctane	17.5	134.4	1.04 ± 0.02
cyclodecane	17.1	164.3	1.02 ± 0.01
benzene	18.7	89.4	1.12 ± 0.02
toluene	18.2	106.9	1.10 ± 0.03
o-xylene	18.4	121.2	1.09 ± 0.01
Tetrahydrofuran*	19.5	81.7	1.14 ± 0.04

* Residual bitumen components dissolved in tetrahydrofuran.

components in petroleum liquids. A suite of liquid hydrocarbons with different number of carbon atoms were selected for each class of solvents. This selection was made to investigate the effect of solvent molecular size and solvent molecular shape on kerogen swelling. Our selection covers a broad range of chain length in normal-alkanes, aliphatic ring size in naphthenes and side methyl group of rings in aromatics. The difference between the three classes of hydrocarbons with the same number of carbon atoms represents the effect of solvent molecular shape. These liquid hydrocarbons cover a wide range of solvent solubility parameter and molar volume at 25 °C (Table 1). In addition to nonpolar solvents, tetrahydrofuran was also selected as a polar solvent to study kerogen swelling.

2.3. Test-tube swelling

Kerogen swelling is a measure of the change in volume of kerogen due to expansion of the organic network by a solvent. To measure swelling, roughly 0.2 g of the extracted kerogen powder was weighed into NMR tubes with outer diameter of 3 mm. NMR tubes are made of glass with uniform thickness. The 3-mm tubes were selected, instead of 5-mm tubes widely used in previous studies [3,6], to improve the accuracy of measurement. The key step in the swelling experiments is to densely pack the kerogen in the NMR tube and then measure the initial kerogen height. Loose packing may result in kerogen shrinkage in solvents if the kerogen swelling is low. Multiple tapping steps were adopted in the kerogen filling process to achieve the highest compaction. The sample tubes were then centrifuged twice at 2500 rpm for 5 min, and the initial height of dry sample was recorded when there was no change in height in hours, which guaranteed sufficient crosslink formation of kerogen network. The crosslinked and elastic properties of kerogen were assumed to be independent of solvent. The liquid hydrocarbons were subsequently added into each tube gradually while tapping, sonication and low speed centrifuging of the sample. This step was expected to squeeze out the air, achieve efficient mixing and minimize the effect of osmotic pressure. Excess solvent was added to ensure that there was 3 to 4 cm of solvent on top of the kerogen in the tube. The tube was placed uprightly for 24 hr, and then centrifuged at 5000 rpm for 5 min before measuring the final height of the sample. The centrifuged step was repeated until there was no change in the final height. The ratio of the final height to the initial height of kerogen is defined as the volumetric swelling ratio. This definition is applicable when the packing density of kerogen remains unchanged. Hruljova et al. [20] have reported the decrease of void volume fraction in swollen kerogen compared with dry kerogen. However, as they emphasized, their results may be caused by either the specific experimental procedure or the kukersite kerogen sample used by them. The underlying causes remain unclear due to the absence of controlled experiments. In this work, we made efforts in the experimental procedure to mitigate the compaction of swollen kerogen. Firstly, multiple tapping steps were performed to achieve the highest compaction of dry kerogen. Secondly, the tube with dry kerogen was kept still for a long time to allow sufficient time in crosslink formation of kerogen network. Thirdly, the solvents were slowly added with tapping, sonication and low speed centrifuging to minimize the effect of osmotic pressure on kerogen structure. With these efforts, it may be plausible to assume that the void volume fraction in kerogen remains unchanged. All measurements were conducted at room temperature and ambient pressure. The measurements were repeated for three times to obtain the mean swelling ratio and standard error.

2.4. Theoretical model

The swelling of kerogen was modeled by the extended regular solution theory framework originally developed for swelling of polymer networks [3]. In this framework, the regular solution theory of Hildebrand [38] is extended by coupling with the Flory-Rehner theory of rubber elasticity [39]. In this treatment, the elastic contribution is integrated in the free energy of the kerogen-solvent system, which, in turn, is utilized to determine the swelling of kerogen network in solvent. The theoretical model has three assumptions [6]: (1) the dissolution of solvent in kerogen is in thermodynamic equilibrium; (2) kerogen network follows a rubber-like behavior; (3) the kerogen-solvent and solvent-solvent interactions are nonspecific. The assumption of rubber-like behavior implies that the amorphous kerogen can experience reversible deformation with exposure to solvent. To possess the rubber-like behavior, the kerogen network may not be over-crosslinked, and the interaction with solvent may not change the crosslinked and elastic properties of kerogen. In the theoretical model, the measured swelling of kerogen in various solvents were used to determine the three thermodynamic parameters of kerogen (solubility parameter, cross-link density, and native swelling fraction), which minimize the overall difference between experimental and theoretical swelling ratios. The solubility parameter represents the degree of interaction in kerogen, and is a measure of solubility [15]. The cross-link density is defined as the density of elastically effective number of chain segments bounded on both ends by crosslinks [6]. Native swelling fraction is equal to the volume fraction of kerogen network that minimizes its elastic strain energy [3]. It reflects the native deformation of kerogen network to reach the unstretched state. The general formulation of the theoretical model has been presented by Ertas et al. [3]for kerogen interaction in multicomponent solvents. In this work, we use the same model for a system in which kerogen interacts with a single excess solvent. Detailed formulation is supplemented in Appendix A.

3. Results

In this section, we report the measured kerogen swelling by normal-alkanes, naphthenes and aromatics (Fig. 2, Table 1). For normal-alkanes, the swelling is measured in n-C_5 to n-C_{10}, n-C_{12} and n-C_{14}. Normal-alkanes with carbon atoms more than 15 are solid at room temperature. The highest kerogen swelling ratio is measured in n-hexane and n-pentane with values of 1.14 ± 0.03 and 1.13 ± 0.01, respectively. As the number of carbon atoms increases in the chain of normal-alkanes, the swelling decreases in the kerogen sample. The averaged swelling in n-C_6 in three measurements is slightly higher than that in n-C_5, but the difference is within the standard deviations. The swelling ratio reaches a plateau for normal-alkanes with the number of carbon atoms higher than 10.

The swelling of kerogen in cycloalkanes is measured for C_5 to C_8,

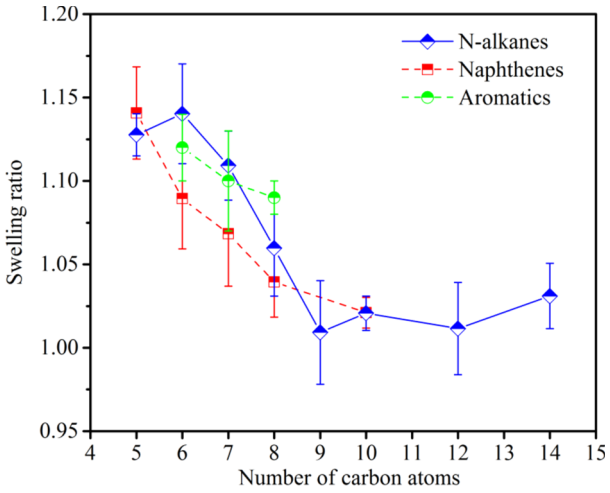

Fig. 2. Swelling ratio of kerogen as a function of number of carbon atoms in different solvents.

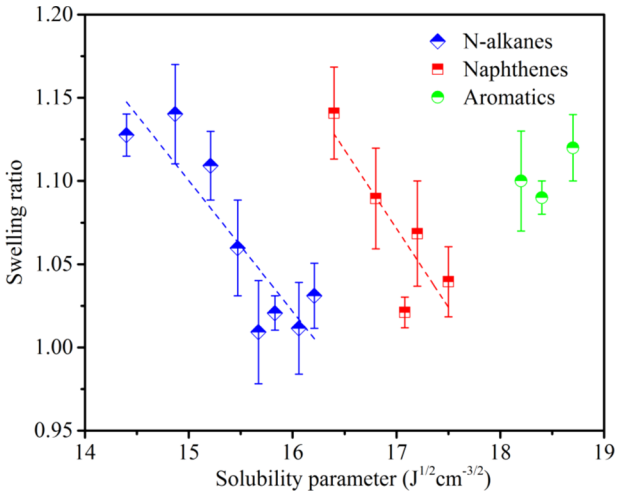

Fig. 3. Swelling ratio of kerogen as a function of solvent solubility parameter in n-alkanes, naphthenes and aromatics. Dashed lines show the trend in n-alkanes and naphthenes.

and C_{10}. The cycloalkanes are solid when the number of carbon atoms is higher than 10. The swelling decreases with the increase in the number of carbon atoms in the ring of naphthenes. The highest swelling ratio of kerogen is 1.14 ± 0.03 in cyclopentane, and the lowest swelling ratio is 1.02 ± 0.01 in cyclodecane. The swelling ratio of kerogen in aromatics is also presented in Fig. 2. A comparison among benzene, toluene and o-xylene in the kerogen sample shows that as the number of methyl groups attached to the base ring increases from zero to two, the swelling ratio decreases slightly from 1.12 ± 0.02 to 1.09 ± 0.01. The swelling ratio of tetrahydrofuran (1.14 ± 0.04) is slightly higher than the aromatic solvents (Table 1). However, we observed the change of color of tetrahydrofuran in the tube as it came in contact with the kerogen sample. This implies that some residual bitumen components dissolve in tetrahydrofuran, since kerogen is insoluble in organic solvent. The dissolution of organic components in solvent can affect the swelling of kerogen, indicating the measured result (1.14 ± 0.04) is most probably not accurate. We exclude tetrahydrofuran for further discussion.

4. Discussion

4.1. Effect of solvent molecular size and shape

Measurements of the three classes of liquid solvents in the Kimmeridge kerogen show a consistent trend; there is a decrease with the increase of solvent molecular size. Specifically, the swelling ratio descends as the chain length increases in normal-alkanes, the ring size expands in naphthenes, and the side methyl group rises in benzene ring of aromatics. This trend is correlated with the size exclusion effect which integrates the fluid molecular size with the pore accessibility in kerogen [41]. The increase in molecular size can reduce the fluid diffusivity in ultraconfining kerogen matrix, which results in less dissolution of fluid. The effect of fluid molecular size is consistent with our recent finding that [17] kerogen swelling induced by water molecules decreases with the increase of kerogen pore sizes. In addition to molecular size for each class of solvents, the comparison of kerogen swelling in the three classes of solvents with the same number of carbon atoms can help to investigate the effect of solvent molecular shape. The kerogen swelling is more pronounced in normal-alkanes with linear chains than that in naphthenes with cyclic rings. This is because the linear molecular chain with flexibility facilitates the fluid to diffuse in the porous channels. Compared with naphthenes, aromatics induce a larger swelling ratio of kerogen, which may be attributed to the π–π interaction between solvents and aromatic rings of kerogen macromolecules [4].

4.2. Effect of solvent solubility parameter and molar volume

Fig. 3 shows the plot of kerogen swelling and solvent solubility parameter. The swelling in normal-alkanes and naphthenes has the same trend; it decreases linearly with the increase of solvent solubility parameter. The two solvent classes have the same slope which is an indication of the type of interaction with the kerogen network. The decreasing linear trend has not been reported in the past to the best of our knowledge. The aromatics are very distinct from alkanes. Previous studies (based on modeling) have reported a bell-shaped [22–24] or increasing trend [6] in different classes of solvents. In this work, the swelling data in different classes of solvents are distinguished with independent trends.

In addition to solvent solubility parameter, solvent molar volume is another key parameter that may correlate with the swelling of kerogen. The swelling of kerogen as a function of solvent molar volume is presented in Fig. 4. The solvent molar volume includes both the effect of solvent molecular size and molecular shape. A decreasing trend of kerogen swelling with increasing solvent molar volume is observed, which confirms the size exclusion effect in the ultraconfining kerogen matrix. The number of solvent molecules that can diffuse into the kerogen matrix diminishes as the solvent molar volume increases.

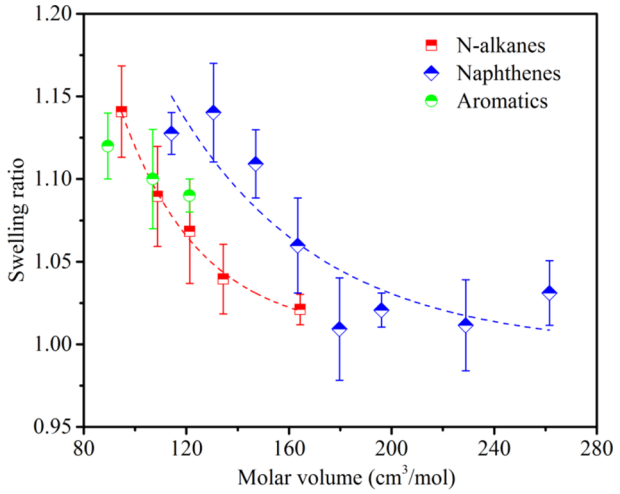

Fig. 4. Swelling ratio of kerogen as a function of solvent molar volume in n-alkanes, naphthenes and aromatics. Dashed lines show the trend in n-alkanes and naphthenes.

Similar to solvent solubility parameter, the dependence of kerogen swelling on solvent molar volume is distinct in normal-alkanes, naphthenes, and aromatics. A comparable exponential trend is observed in the two classes of alkanes, which demonstrates the interactions are similar.

In Figs. 3 and 4, the swelling data of aromatics show a different class and trend. Due to small range in solubility parameter and molar volume in the three aromatics, a definitive trend cannot be deduced.

In Fig. 2, the swelling of Kimmeridge kerogen reveals a decreasing trend as the molar volume of solvent increases and the solubility parameter of solvent gets closer to the general kerogen solubility parameter [3,6,22–24]. It is assumed that the swelling increases when the solubility parameter of solvent approaches that of kerogen. Compared with solvent solubility parameter, the molar volume of solvent dominates the swelling of Kimmeridge kerogen. Hruljova et al. [20] have also reported that the solubility parameter of solvent may not be a key parameter, while the molar volume of solvent could be a dominate parameter in determining the swelling of Kukersite kerogen. In their work, the kerogen swelling showed no clear relation with solvent solubility parameter and a linear trend was not observed with solvent molar volume.

4.3. Description by the extended regular solution theory framework

The extended regular solution theory framework has been used in the past to describe kerogen swelling by various authors [3,6]. Fig. 1 was prepared based on the three coefficients which were obtained from swelling measurements of alkanes and aromatics in ref [6]. As the figure shows the kerogen swelling increases with the increase in the number of carbon atoms in normal-alkanes. This theoretical trend is contrary to the experimental trend in Fig. 2. In this work, our goal is investigation of the applicability of the extended regular solution theory to the swelling of Kimmeridge kerogen in petroleum liquids. We will demonstrate that although the theoretical predictions can match well with the experimental results, the predictions are based on fitting of the three thermodynamic parameters of kerogen, and the fitting thermodynamics parameters especially the fitted solubility parameter of kerogen may not have a sound physical meaning.

The swelling ratio of kerogen in the three class of hydrocarbons from our measurements is modeled and presented in Fig. 5. We have used all of our data together (Fig. 5 a) and then all the data for n-alkanes and naphthenes (Fig. 5 b) and then separately (Fig. 5 c, d) to get the parameters of the model. The theoretical predictions for swelling ratio of kerogen in normal-alkanes and naphthenes match well with the experimental data (Fig. 5 b–d). In contrast, the theoretical results for aromatics are different from the experimental data (Fig. 5 a). This observation indicates that aromatics may have different interactions with the kerogen network compared with normal-alkanes and naphthenes. The difference can be due to the π–π interaction between aromatics and kerogen aromatic units [4].

Fig. 6 presents the theoretical predictions of kerogen swelling ratio as a function of solvent solubility parameter and molar volume based on experimental results of normal-alkanes and naphthenes. The swelling follows a bell-shaped trend with the solvent solubility parameter, which first increases to a maximum, and then decreases with further increase in solubility parameter. The bell-shaped trend is consistent with the reported experimental results for type I and III kerogen [23]. Note that the theoretical swelling shows a decreasing trend as the solvent solubility parameter varies from 14.4 to 18.7 $J^{1/2}cm^{-3/2}$, which is in qualitative agreement with the experimental data. The solvent solubility parameter is well defined. In contrast, the solubility parameter of kerogen cannot be measured directly. It is estimated from the swelling measurements. The kerogen solubility parameter has been reported to vary between 19 and 24.3 $J^{1/2}cm^{-3/2}$ [3,6,22–24], which is close to that of petroleum asphaltenes [35]. Table 2 presents the solubility parameter of kerogen based on description of the extended regular solution theory and our data. The solubility parameters are obtained from all of our data, as well as separating the data in different classes of solvents. Note that the kerogen solubility parameters in Table 2 are less than the solubility parameters of light liquid normal alkanes in Table 1; they are much less than the kerogen solubility parameters reported in the literature. As we have seen above there is inconsistency in the predictions from the literature solubility parameters with the trends of our normal alkane data. The other two parameters of the extended regular solution theory are in qualitative agreement with the values obtained in the past.

Going back to Fig. 5, we observe that the kerogen swelling from the extended regular solution theory matches the experimental results (except for aromatics). However, the thermodynamics parameters especially the solubility parameter may not have a sound physical meaning. The cross-link density is reported to increase with the poly-aromatic clusters in kerogen, which increases as the thermal maturity of kerogen from immature to overmature [42] or as the organic type of kerogen changes from type I, type II to type III [43]. The cross-link density (0.10–0.15 mol/cm^3) for Kimmeridge kerogen (type II) from our work is lower than the reported results for type II kerogen (0.16 mol/cm^3) and type IIIC kerogen (0.25 mol/cm^3) [6]. The solubility parameter of kerogen in Table 2 (8.5–10.8 $J^{1/2}cm^{-3/2}$) is two times less than the values (19–24.3 $J^{1/2}cm^{-3/2}$) in the literature [3,6,22–24]. The large difference indicates that the extended Flory-Rehner and regular solution theory may not describe the swelling of kerogen.

The theoretical model can fit the measured swelling of Kimmeridge kerogen by adjusting the thermodynamic parameters of kerogen, but the optimized solubility parameter does not have a sound thermodynamic basis. Therefore, the theoretical model may not describe the swelling of Kimmeridge kerogen in petroleum liquids. Oja et al. [44] have reported a similar conclusion but from a different aspect. They concluded that the extended Flory-Rehner and regular solution theory is not suitable for Green River kerogen, because the average molecular weights between cross-links predicted by the theoretical model were clearly lower than the experimentally determined results. These observations indicate that the extended Flory-Rehner and regular solution theory may not be reliable for quantitative estimate, which can be attributed to the uncertainties in the assumptions and simplifications of the theoretical model. In addition to an enthalpic term, the kerogen-solvent interaction parameter can also contribute to an entropic term. The neglect of the entropic term in the theoretical model may increase the uncertainty. Furthermore, the theoretical model requires the kerogen to follow the rubber-like behavior, namely the interaction with solvent does not change the crosslinked and elastic properties of kerogen, which may be invalid for realistic kerogen samples with highly irregular structural segments and heterogeneous nature.

5. Conclusions

We draw two main conclusions from this investigation.

1. Kerogen swelling decreases as the chain length increases in normal-alkanes, the ring size expands in naphthenes, and the side methyl group increases in benzene ring of aromatics. Compared with naphthenes with cyclic rings, the swelling is higher in normal-alkanes with flexible linear chains and in aromatics having π–π interaction with kerogen.
   The swelling ratio of Kimmeridge kerogen in both normal-alkanes and naphthenes shows a linear decrease with the solvent solubility parameter and an exponential decrease with the solvent molar volume. The swelling in the two classes of alkanes has a similar decreasing slope, demonstrating similar interactions with the kerogen network. Compared with solvent solubility parameter, the effect of solvent molar volume dominates the swelling of kerogen in normal-alkanes and naphthenes.

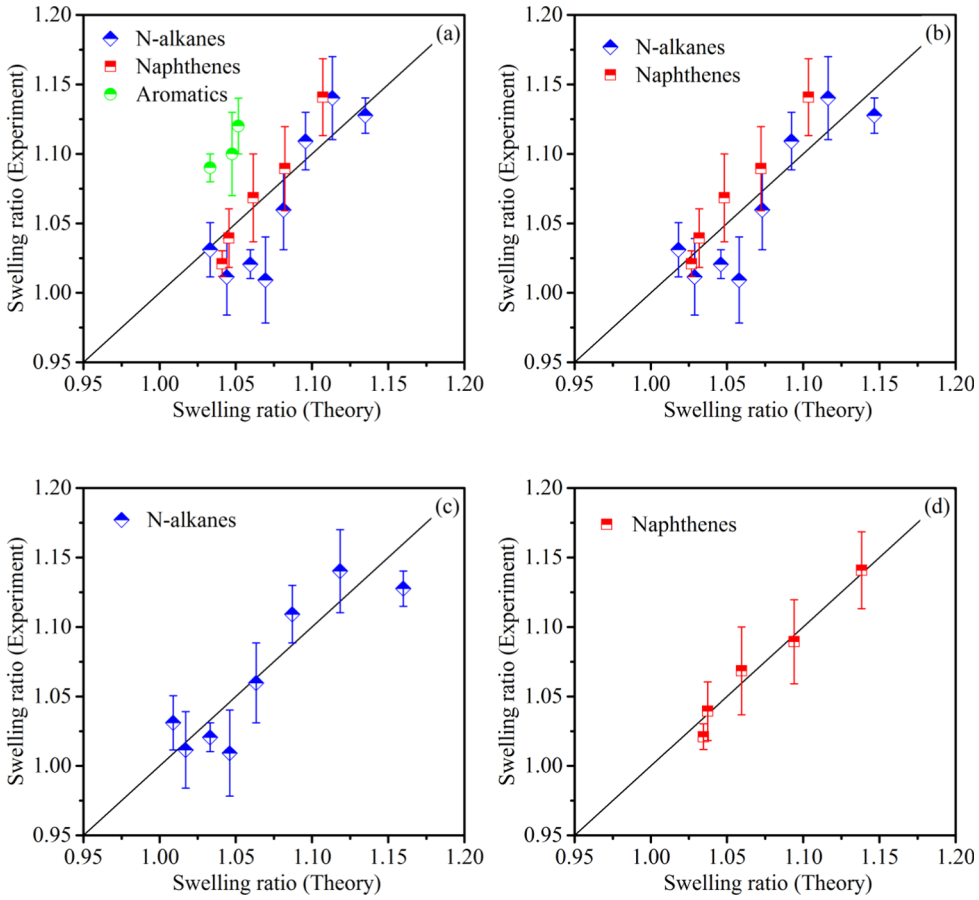

Fig. 5. Kerogen swelling ratio from experiments and description by the extended regular solution theory: (a) normal alkanes, naphthenes and aromatics; (b) normal alkanes and naphthenes; (c) normal alkanes; (d) naphthenes.

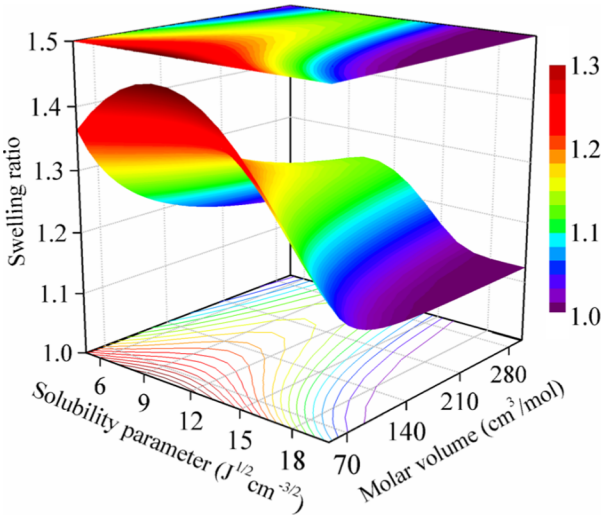

Fig. 6. Kerogen swelling ratio from theoretical predictions as a function of solvent solubility parameter and molar volume. The theoretical predictions are based on the thermodynamic parameters for kerogen from an optimum fit of experimental data of alkanes. The bottom plots correspond to the contour surface, the middle plots correspond to the three-dimensional surface, and the top plots correspond to the projection of the surface of the middle plots.

2. The extended Flory-Rehner and regular solution theory framework may not describe the swelling of kerogen in petroleum liquids. The optimized thermodynamic parameters of kerogen do not have a sound thermodynamic basis. Alternative models may be pursued in the future.

Table 2
Thermodynamic parameters for kerogen from an optimum fit of our experimental data in the thermodynamic model.

Solvent	Solubility parameter ($J^{1/2}cm^{-3/2}$)	Cross-link density (mol/cm^3)	Native swelling fraction
Alkanes + Aromatics	10.8	0.15	0.95
Alkanes	10.3	0.10	0.95
N-alkanes	8.5	0.10	0.85
Naphthenes	8.8	0.10	0.80

CRediT authorship contribution statement

Liang Huang: Data creation, Formal analysis, Validation, Visualization, Writing - original draft, Writing - review & editing. **Atefeh Khoshnood:** Investigation, Methodology, Writing - original draft. **Abbas Firoozabadi:** Conceptualization, Funding acquisition, Project administration, Supervision, Writing - review & editing.

Declaration of Competing Interest

The authors declare that they have no known competing financial interests or personal relationships that could have appeared to influence the work reported in this paper.

Acknowledgments

This work was supported by the member companies of the Reservoir Engineering Research Institute (RERI). We appreciate the support of the

National Natural Science Foundation of China (Grant No. 51774298) and the China Scholarship Council (CSC No. 201806440095). We would like to thank Mr. Peng Gao of Stanford University for his help on programming the extended Regular Solution Theory. We also thank Dr. Tianhao Wu and Dr. Ali Zidane of RERI for discussion.

Appendix A

One key relationship is the expression for the change in Gibbs free energy of the system which includes entropic and enthalpic terms. The changes in entropy originate from two sources: conformational variations and entropy of mixing. According to Flory-Rehner theory, an affine transformation in the network of a crosslinked polymer results in the following entropic changes [38],

$$\Delta S_c = -k_B \frac{N_e}{2}[\alpha_x^2 + \alpha_y^2 + \alpha_z^2 - 3 - 2\ln(\alpha_x\alpha_y\alpha_z)] \tag{1}$$

In Eq. (1), ΔS_c is the change in entropy due to conformational variations, k_B is the Boltzmann constant, α_x, α_y, α_z are the fractional elongations along the x, y, and z directions, respectively, N_e is the elastically effective number of chain segments bounded on both ends by crosslinks. N_e is defined as the total number of crosslinked units minus the number of terminal chains bounded at one end to a cross-linkage [38]. The terminal chains have no contribution to the elastic free energy.

By introducing native swelling fraction υ_{eq}, kerogen volume fraction υ_0, and assuming uniform elongation $\alpha_x = \alpha_y = \alpha_z = (\upsilon_{eq}/\upsilon_0)^{1/3}$, Eq. (1) can be rewritten as,

$$\Delta S_c = -k_B \frac{N_e}{2}\left[3\left(\frac{\upsilon_{eq}}{\upsilon_0}\right)^{\frac{2}{3}} - 3 - 2\ln\left(\frac{\upsilon_{eq}}{\upsilon_0}\right)\right] \tag{2}$$

where υ_0 is the kerogen volume fraction, υ_{eq} is the native swelling fraction. The native swelling fraction υ_{eq} is numerically equal to the volume fraction of kerogen network that minimizes its elastic strain energy [3]. The native swelling fraction υ_{eq} is an innate thermodynamic parameter of kerogen network, which is independent of solvent type and amount.

The entropy of mixing is given by [3],

$$\Delta S_m = -k_B n_1 \ln \upsilon_1 \tag{3}$$

where ΔS_m is the change in entropy due to introduction of solvent, n_1 and υ_1 are the total number of solvent molecules and solvent volume fraction, respectively. Eq. (3) can be used to interpret the mixtures of kerogen and solvent when ignoring specific interactions. In this equation, the solute term is excluded since the equation is utilized to describe the contribution of solvent introduction to the associated change of conformational entropy. The contribution of solute to the change of conformational entropy is described in Eq. (2).

The heat exchange due to mixing of solvent and kerogen network can be obtained by [3],

$$\Delta H_m = k_B T \chi_{1,0} n_1 \upsilon_0 \tag{4}$$

where ΔH_m is the change in enthalpy due to mixing of solvent and kerogen, $\chi_{1,0}$ is the interaction parameter between solvent (1) and kerogen network (0), and T is temperature. An alternative way of writing Eq. (4) is by defining interaction energy density $b_{1,0} = \chi_{1,0}/\theta$, where θ is the molecular volume of the solvent. The molecular volume is converted from the molar volume of solvent [15,40], divided by Avogadro constant.

We can relate the enthalpy of mixing to solubility parameters through the regular solution theory [38],

$$b_{1,0} = \frac{(\delta_1 - \delta_0)^2}{k_B T} \tag{5}$$

where $b_{1,0}$ is interaction energy, δ_1 and δ_0 are solubility parameters of solvent and kerogen, respectively.

The change in Gibbs free energy from mixing of kerogen and solvent molecules is given by,

$$\Delta G = \Delta H_m - T(\Delta S_m + \Delta S_c) \tag{6}$$

where ΔG is the change in Gibbs free energy. By substituting Eqs. (2), (3), (4), (5) into Eq. (6), we arrive at,

$$\frac{\Delta G}{k_B T} = b_{1,0}\theta n_1 \upsilon_0 + n_1 \ln \upsilon_1 + \frac{N_e}{2}\left[3\left(\frac{\upsilon_{eq}}{\upsilon_0}\right)^{\frac{2}{3}} - 3 - 2\ln\left(\frac{\upsilon_{eq}}{\upsilon_0}\right)\right] \tag{7}$$

The expression for ΔG can be used to calculate the chemical potentials. The change in chemical potential of the solvent in contact with kerogen network with reference to pure liquid is,

$$\frac{\Delta \mu_1}{k_B T} = \frac{1}{k_B T}\frac{\partial \Delta G}{\partial n_1} \tag{8}$$

where $\Delta\mu_1$ is the change in chemical potential of the solvent. By substituting Eq. (7) into Eq. (8) and carrying out the derivative, we arrive at,

$$\frac{\Delta \mu_1}{k_B T} = b_{1,0}\theta \upsilon_0^2 + \ln \upsilon_1 + \upsilon_0 + \frac{N_e \theta}{\omega}\left(\upsilon_0^{\frac{1}{3}}\upsilon_{eq}^{\frac{2}{3}} - \upsilon_0\right) \tag{9}$$

where ω is the initial volume occupied by the kerogen network, and υ_1 is the solvent volume fraction ($\upsilon_1 = 1 - \upsilon_0$). The kerogen volume fraction in the mixture is defined as $\upsilon_0 = \omega/(\omega + n_1\theta)$. The volumetric swelling ratio is the inverse of the kerogen volume fraction, $Q_v = \upsilon_0^{-1}$. Now we write the equilibrium condition for the liquid absorbed in the kerogen network and the excess liquid. The swelling is modeled similar to the way the experiments are performed; there is always excess solvent after equilibrium has been reached. Therefore, $\Delta\mu_1^{(absorbed)} = \Delta\mu_1^{(excess)}$. Note that the theoretical model ignores the effect of osmotic pressure on solvent partitioning and kerogen swelling. We can write the working equation for kerogen swelling calculations,

$$b_{1,0}\theta v_0^2 + \ln(1 - v_0) + v_0 + \frac{N_e\theta}{\omega}\left(v_0^{\frac{1}{3}} v_{eq}^{\frac{2}{3}} - v_0\right) = 0 \tag{10}$$

Eq. (10) can be used to calculate kerogen swelling by excess solvent once we determine the three thermodynamic parameters of kerogen (solubility parameter δ_0, native swelling fraction v_{eq} and crosslink density N_e/ω). Note that the three thermodynamic parameters reflect the innate properties of kerogen network, which are independent of solvent type and amount. In this treatment, the three thermodynamic parameters are first determined by optimizing the match of the swelling data and the theoretical model. For this purpose, a cost function ξ is defined to minimize the error of predictions and experiments [3,6],

$$\zeta = \frac{\sum_{i=1}^{N} [(Q_v)_i^p - (Q_v)_i^e]^2}{\sum_{i=1}^{N} [(Q_v)_i^e]^2 - \frac{1}{N}\left[\sum_{i=1}^{N} (Q_v)_i^e\right]^2} \tag{11}$$

In Eq. (11), ξ is the cost function, and N is the number of data points. Superscript p and e refer to predicted and experimental results, respectively. In this work, we adopt the traversing method to find the combination of the three parameters that leads to the minimized cost function. The search region is 0–40 $J^{1/2}cm^{-3/2}$ for solubility parameter of kerogen, 0–1 mol/cm^3 for crosslink density of kerogen and 0–1 for native swelling fraction. In this method, all the possible combinations of the three parameters are examined to ensure that the optimized combination is obtained.

References

[1] Bousige C, Ghimbeu CM, Vix-Guterl C, Pomerantz AE, Suleimenova A, Vaughan G, et al. Realistic molecular model of kerogen's nanostructure. Nat Mater 2016;15(5):576–82.
[2] Sert M, Ballice L, Yüksel M, Saglam M, Reimert R, Erdem S. Effect of solvent swelling on pyrolysis of kerogen (type-I) isolated from Göynük oil shale (Turkey). J Anal Appl Pyrol 2009;84(1):31–8.
[3] Ertas D, Kelemen SR, Halsey TC. Petroleum expulsion part 1. Theory of kerogen swelling in multicomponent solvents. Energy Fuels 2006;20(1):295–300.
[4] Huang L, Ning Z, Wang Q, Qi R, Li J, Zeng Y, et al. Thermodynamic and structural characterization of bulk organic matter in Chinese Silurian shale: experimental and molecular modeling studies. Energy Fuels 2017;31(5):4851–65.
[5] Huang L, Ning Z, Wang Q, Ye H, Wang Z, Sun Z, et al. Microstructure and adsorption properties of organic matter in Chinese Cambrian gas shale: Experimental characterization, molecular modeling and molecular simulation. Int J Coal Geol 2018;198:14–28.
[6] Kelemen SR, Walters CC, Ertas D, Kwiatek LM, Curry DJ. Petroleum expulsion part 2. Organic matter type and maturity effects on kerogen swelling by solvents and thermodynamic parameters for kerogen from regular solution theory. Energy Fuels 2006;20(1):301–8.
[7] Kelemen SR, Walters CC, Ertas D, Freund H, Curry DJ. Petroleum expulsion part 3. A model of chemically driven fractionation during expulsion of petroleum from kerogen. Energy Fuels 2006;20(1):309–19.
[8] Jin Z, Firoozabadi A. Thermodynamic modeling of phase behavior in shale media. SPE J 2016;21(01):190–207.
[9] Liu J, Chapman WG. Thermodynamic modeling of the equilibrium partitioning of hydrocarbons in nanoporous kerogen particles. Energy Fuels 2019;33(2):891–904.
[10] Pathak M, Kweon H, Deo M, Huang H. Kerogen swelling and confinement: its implication on fluid thermodynamic properties in shales. Sci Rep-UK 2017;7(1):12530.
[11] Sandvik EI, Young WA, Curry DJ. Expulsion from hydrocarbon sources: the role of organic absorption. Org Geochem 1992;19(1–3):77–87.
[12] Sandvik EI, Mercer JN. Primary migration by bulk hydrocarbon flow. Org Geochem 1990;16(1–3):83–9.
[13] Thomas MM, Clouse JA. Primary migration by diffusion through kerogen: III. Calculation of geologic fluxes. Geochim Cosmochim Ac 1990;54(10):2793–7.
[14] Ritter U. Fractionation of petroleum during expulsion from kerogen. J Geochem Explor 2003;78:417–20.
[15] Ritter U. Solubility of petroleum compounds in kerogen: implications for petroleum expulsion. Org Geochem 2003;34(3):319–26.
[16] Wu T, Firoozabadi A. Effect of Microstructural flexibility on methane flow in kerogen matrix by molecular dynamics simulations. J Phys Chem C 2019;123(17):10874–80.
[17] Huang L, Ning Z, Wang Q, Qi R, Cheng Z, Wu X, et al. Molecular insights into kerogen deformation induced by CO_2/CH_4 sorption: effect of maturity and moisture. Energy Fuels 2019;33(6):4792–805.
[18] Tesson S, Firoozabadi A. Methane adsorption and self-diffusion in shale kerogen and slit nanopores by molecular simulations. J Phys Chem C 2018;122(41):23528–42.
[19] Hruljova J, Savest N, Oja V, Suuberg EM. Kukersite oil shale kerogen solvent swelling in binary mixtures. Fuel 2013;105:77–82.
[20] Hruljova J, Järvik O, Oja V. Application of differential scanning calorimetry to study solvent swelling of kukersite oil shale macromolecular organic matter: A comparison with the fine-grained sample volumetric swelling method. Energy Fuels 2014;28(2):840–7.
[21] Hruljova J, Oja V. Application of DSC to study the promoting effect of a small amount of high donor number solvent on the solvent swelling of kerogen with non-covalent cross-links in non-polar solvents. Fuel 2015;147:230–5.
[22] Larsen JW, Li S. Solvent swelling studies of Green River kerogen. Energy Fuels 1994;8(4):932–6.
[23] Larsen JW, Li S. An initial comparison of the interactions of Type I and III kerogens with organic liquids. Org Geochem 1997;26(5–6):305–9.
[24] Larsen JW, Parikh H, Michels R. Changes in the cross-link density of Paris Basin Toarcian kerogen during maturation. Org Geochem 2002;33(10):1143–52.
[25] Ballice L, Larsen JW. Changes in the cross-link density of Goynuk oil shale (Turkey) on pyrolysis. Fuel 2003;82(11):1305–10.
[26] Savest N, Oja V, Kaevand T, Lille Ü. Interaction of Estonian kukersite with organic solvents: A volumetric swelling and molecular simulation study. Fuel 2007;86(1–2):17–21.
[27] Savest N, Hruljova J, Oja V. Characterization of thermally pretreated kukersite oil shale using the solvent-swelling technique. Energy Fuels 2009;23(12):5972–7.
[28] Kilk K, Savest N, Hruljova J, Tearo E, Kamenev S, Oja V. Solvent swelling of dictyonema. Oil Shale 2010;27(1):26–36.
[29] Chen Z, Singer PM, Kuang J, Vargas FM, Hirasaki GJ. Effects of bitumen extraction on the 2D NMR response of saturated kerogen isolates. Petrophysics 2017;58(05):470–84.
[30] Painter PC, Shenoy SL. A simple model for the swelling of polymer networks. J Chem Phys 1993;99(2):1409–18.
[31] Paik JS, Tigani MA. Application of regular solution theory in predicting equilibrium sorption of flavor compounds by packaging polymers. J Agr Food Chem 1993;41(5):806–8.
[32] Painter PC, Graf J, Coleman MM. Coal solubility and swelling. 1. Solubility parameters for coal and the Flory. chi. parameter. Energy Fuels 1990;4(4):379–84.
[33] Chen C, Gao J, Yan Y. Role of noncovalent bonding in swelling of coal. Energy Fuels 1998;12(6):1328–34.
[34] Nikooyeh K, Shaw JM. On the applicability of the regular solution theory to asphaltene+ diluent mixtures. Energy Fuels 2012;26(1):576–85.
[35] Dechaine GP, Maham Y, Tan X, Gray MR. Regular solution theories are not appropriate for model compounds for petroleum asphaltenes. Energy Fuels 2011;25(2):737–46.
[36] Kiselev AV. Non-specific and specific interactions of molecules of different electronic structures with solid surfaces. Discuss Faraday Soc 1965;40:205–18.
[37] Zhao H, Lai Z, Firoozabadi A. Sorption hysteresis of light hydrocarbons and carbon dioxide in shale and kerogen. Sci Rep-UK 2017;7(1):16209.
[38] Hildebrand JH, Prausnitz JM, Scott RL. Regular and Related Solutions, • Van Nostrand Reinhold. New York, NY 1970.
[39] Flory PJ, JrJ Rehner. Statistical mechanics of cross-linked polymer networks I. Rubberlike elasticity. J Chem Phys 1943;11(11):512–20.
[40] Barton AFM. Handbook of Solubility Parameters and Other Cohesion Parameters. Boca Raton, FL: CRC Press; 1983.
[41] Falk K, Pellenq R, Ulm FJ, Coasne B. Effect of chain length and pore accessibility on alkane adsorption in kerogen. Energy Fuels 2015;29(12):7889–96.
[42] Huang L, Ning Z, Wang Q, Qi R, Zeng Y, Qin H, et al. Molecular simulation of adsorption behaviors of methane, carbon dioxide and their mixtures on kerogen: Effect of kerogen maturity and moisture content. Fuel 2018;211:159–72.
[43] Huang L, Ning Z, Wang Q, Zhang W, Cheng Z, Wu X, et al. Effect of organic type and moisture on CO_2/CH_4 competitive adsorption in kerogen with implications for CO_2 sequestration and enhanced CH_4 recovery. Appl Energy 2018;210:28–43.
[44] Oja V. Examination of molecular weight distributions of primary pyrolysis oils from three different oil shales via direct pyrolysis Field Ionization Spectrometry. Fuel 2015;159:759–65.